

Hidden States as Early Signals: Step-level Trace Evaluation and Pruning for Efficient Test-Time Scaling

Zhixiang Liang*, Beichen Huang*, Zheng Wang, Minjia Zhang

University of Illinois Urbana-Champaign

{zliang18, beichen8, zhengw10, minjiaz}@illinois.edu

Abstract

Large Language Models (LLMs) can enhance reasoning capabilities through test-time scaling by generating multiple traces. However, the combination of lengthy reasoning traces with multiple sampling introduces substantial computation and high end-to-end latency. Prior work on accelerating this process has relied on similarity-based or confidence-based pruning, but these signals do not reliably indicate trace quality. To address these limitations, we propose **STEP**: Step-level Trace Evaluation and Pruning, a novel pruning framework that evaluates reasoning steps using hidden states and dynamically prunes unpromising traces during generation. We train a lightweight step scorer to estimate trace quality, and design a GPU memory-aware pruning strategy that triggers pruning as the GPU memory is saturated by KV cache to reduce end-to-end latency. Experiments across challenging reasoning benchmarks demonstrate that STEP reduces end-to-end inference latency by 45%–70% on average compared to self-consistency while also improving reasoning accuracy. Our code is released at: <https://github.com/Supercomputing-System-AI-Lab/STEP>

1 Introduction

Large Language Models (LLMs) have demonstrated exceptional reasoning capabilities, particularly through test-time scaling (TTS) techniques that allocate additional computation during inference (Wei et al., 2022; Kojima et al., 2023; OpenAI, 2024a; DeepSeek-AI, 2025; Hou et al., 2025). Among these methods, self-consistency (Wang et al., 2022) is the most widely adopted parallel scaling approach, which generates multiple traces and selects the final answer through majority voting, repeatedly achieving state-of-the-art performance on reasoning tasks (OpenAI, 2024b). However, both lengthy reasoning traces and multiple

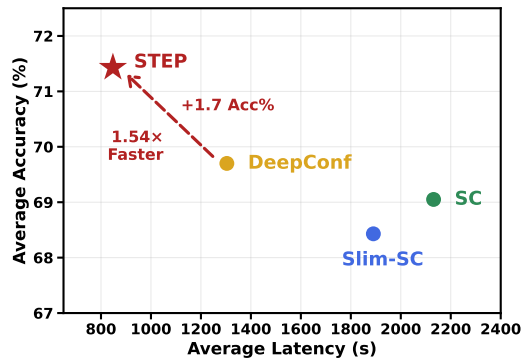


Figure 1: Comparison of accuracy versus latency across different methods on DeepSeek-R1-0528-Qwen3-8B. STEP achieves superior accuracy (averaged across AIME-25, HMMT-24/25, GPQA-D) while significantly reducing latency compared to baseline methods.

sampling paths contribute to prohibitive computational costs and substantial latency, severely limiting their practical deployment (Wang et al., 2025; Ji et al., 2025). Furthermore, self-consistency treats all reasoning trajectories equally, wasting resources on erroneous traces that fail to contribute to the correct answer (Hong et al., 2025).

Prior work to speedup parallel scaling focuses on pruning low-quality traces during the reasoning process, but faces two fundamental limitations. First, the signals used to evaluate trace quality are unreliable. One line of methods prunes similar reasoning traces to preserve answer diversity (Hong et al., 2025; Tu et al., 2025). This is problematic since multiple valid paths can converge to the same correct answer, and surface-level textual similarity does not necessarily indicate redundancy in reasoning quality. Another line of methods leverages the LLM’s internal confidence for early stopping (Fu et al., 2025; Kang et al., 2025), assuming high confidence correlates with correctness. However, confidence scores do not reliably indicate correctness, as models can exhibit high confidence even for factually false or logically inconsistent outputs,

*Equal contribution.

which is known as miscalibration (Chhikara, 2025).

Second, existing approaches overlook a critical factor: the dominant bottleneck of end-to-end latency lies not only in the number of generated tokens, but also in the inference system design and its interaction with the algorithm. By focusing primarily on reducing token generation, these methods can yield speedups but fail to fully address the latency bottleneck. When applying parallel scaling methods to complex reasoning tasks, the KV cache of multiple long traces can rapidly exhaust GPU memory. Once the pre-allocated KV cache memory becomes insufficient, inference systems typically preempt traces into a waiting queue until others complete (Kwon et al., 2023). We observe that these waiting periods, together with the resulting redundant computation, constitute the primary end-to-end latency bottleneck.

To address these limitations, we propose **STEP**: **S**tep-level **T**race **E**valuation and **P**runing, a novel pruning method that leverages the hidden state to evaluate the trace quality during generation and trigger pruning with GPU memory awareness. Our approach is motivated by two insights from preliminary experiments. First, hidden states at reasoning step boundaries encode rich information about the model’s reasoning dynamics (Yang et al., 2025b), making them suitable for quality assessment. Second, these signals emerge early: hidden states from early reasoning steps are already sufficient to distinguish promising traces from unpromising ones. Based on these insights, we train a lightweight step scorer on step boundary hidden states, enabling early assessment of reasoning quality with negligible overhead and allowing us to precisely halt unpromising responses.

Beyond algorithmic design, we additionally consider efficiency from an inference system perspective, which has been largely overlooked by prior work. We leverage GPU memory utilization as the signal to trigger pruning. As KV cache accumulation drives GPU memory toward saturation, we prune the least promising trace and immediately release its resources, preventing preemption and queuing delays. By accounting for this system-level bottleneck, our design reduces unnecessary computation and eliminates memory-induced waiting overhead, substantially improving end-to-end generation latency.

We evaluate STEP across challenging reasoning benchmarks (AIME-25, HMMT-24/25, GPQA-Diamond) and models at different scales

(Qwen3-4B-Thinking-2507, DeepSeek-R1-0528-Qwen3-8B, Phi-4-reasoning-plus(14B)). Experiments demonstrate that STEP reduces end-to-end inference latency by 45%–70% on average compared to self-consistency while also improving reasoning accuracy by +0.4 to +7.5 percentage points. These gains benefit from both the hidden-state-based early pruning and the GPU-memory-aware system optimization, highlighting the potential of efficient test-time scaling to advance complex reasoning capabilities in LLMs.

2 Related Work

2.1 Trace Pruning for Parallel Scaling

Recent work on accelerating parallel scaling has explored pruning unpromising traces during generation. These methods fall into two categories: confidence-based methods that prune low-confidence traces (Fu et al., 2025; Zhou et al., 2025), and diversity-based methods that remove similar traces to preserve answer diversity (Hong et al., 2025; Tu et al., 2025). However, both approaches have notable limitations: confidence scores can suffer from model overconfidence and miscalibration (Chhikara, 2025), while surface-level similarity does not necessarily indicate reasoning redundancy, risking the inadvertent removal of correct traces. And these primarily aim at reducing the average generated tokens per question to accelerate reasoning process, which neglects the system perspective that fundamentally slows down the generation.

2.2 Hidden-state as Reasoning Evaluator

Assessing reasoning trace quality is critical for enhancing the reliability of LLMs in parallel scaling. Recent studies have investigated using LLM internal representations to assess reasoning quality. Zhang et al. (2025) show that reasoning models encode correctness-related information in their hidden states and that a lightweight probe can predict whether an intermediate answer is correct. CLUE (Liang et al., 2025) proposes a non-parametric verifier that clusters hidden-state features from past experience and predicts correctness by comparing a candidate trace’s hidden-state signature to success/failure centroids, demonstrating that hidden states provide a strong correctness signal and can improve final selection. Building on these findings, we identify step boundaries as natural checkpoints where hidden states provide clear quality signals.

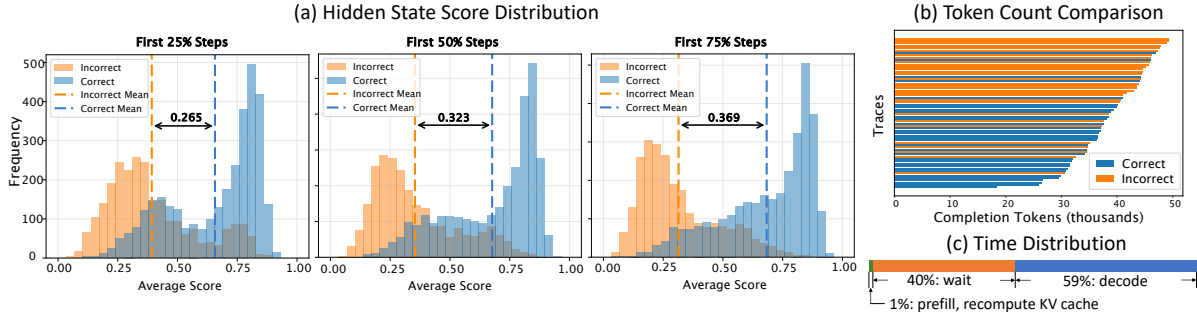


Figure 2: (a) Hidden state score distributions for correct vs. incorrect reasoning traces on HMMT-25. Scores are computed by the scorer model as averages over the first 25%, 50%, and 75% of reasoning steps. (b) Token count comparison of correct and incorrect traces for AIME-25 Q28 using Qwen3-4B-Thinking-2507; incorrect traces average 42.5k tokens compared to 35.3k for correct ones. (c) Time distribution for generating one trace on the same setup; waiting time (59%) dominates over actual decoding (40%), with KV cache reconstruction accounting for 1%.

We train a lightweight step scorer on these boundary representations, enabling continuous monitoring and early pruning in parallel scaling.

3 Motivation

As discussed above, current parallel scaling methods face two key challenges: difficulty in distinguishing correct reasoning traces from incorrect ones and high end-to-end latency. In our preliminary experiments, we find that the hidden states of reasoning models contain rich signals indicative of reasoning quality, and we identify the primary source of the latency bottleneck in parallel scaling.

Discriminative Signals in Hidden States Recent studies (Zhang et al., 2025; Liang et al., 2025) have shown that the hidden states of completed reasoning traces can serve as a reliable proxy for assessing reasoning quality. Our preliminary experiments further demonstrate that hidden states from early reasoning steps are already information-rich and provide a strong signal for reasoning correctness. As illustrated in Fig. 2a, we train a simple 2-layer MLP on hidden states to predict reasoning correctness. We find that the hidden state score from early steps effectively distinguishes between correct and incorrect reasoning paths, with higher scores indicating a greater likelihood of correctness, and the discriminability becomes stronger as reasoning progresses. These findings indicate that internal signals can efficiently assess reasoning quality during generation, motivating our use of hidden states for early trace pruning.

Latency Bottleneck in Parallel Scaling We observe two main sources of inefficiency in parallel scaling. First, incorrect traces tend to be longer

than correct ones as shown in Fig. 2b. Early termination of such traces can eliminate the token generated for each question, therefore improving both efficiency and accuracy. Second, we observe a more fundamental bottleneck arising from inference system behavior, which has been largely overlooked by prior work. As generation progresses, KV cache accumulation quickly saturates GPU memory. When this happens, the inference engine (e.g., vLLM (Kwon et al., 2023), SGLang (Zheng et al., 2024)) preempts traces in waiting queue and frees or offloads its KV cache to allow further generation. Once a trace naturally finishes generation and releases its KV cache, a waiting trace can be resumed, with its KV cache reconstructed before generation continues. As shown in Fig. 2c, waiting time accounts for approximately 59% of end-to-end latency, while actual decoding occupies only 40%. These observations motivate a pruning strategy that explicitly accounts for inference system.

4 STEP

In this section, we progressively construct STEP. Designing an effective pruning method involves two key questions: **which reasoning traces to prune** and **when pruning should be triggered**. As illustrated in the overview in Fig. 3, STEP addresses the first question with a step scorer that evaluates every step during generation, and the second with a KV cache-aware monitoring mechanism. We next describe each component in detail by systematically answering these two questions.

4.1 Step Scorer

As discussed in the Section 3, we train a step scorer that leverages hidden-state representations to assess



Question: Two points are chosen uniformly at random inside a regular hexagon. What is the probability that the line through the two points intersects two opposite sides of the hexagon?

Trace 1: I can try to solve by using symmetry.
Wait, I think a better approach, let's consider the set of lines that intersect that pair.

Trace 2: Let's try to set up coordinate system for hexagon.
I think each chord corresponds uniquely to a line that intersects the hexagon.

Trace 3: So let's fix coordinate system.
And maybe I can compute using the idea of random chords in a circle.

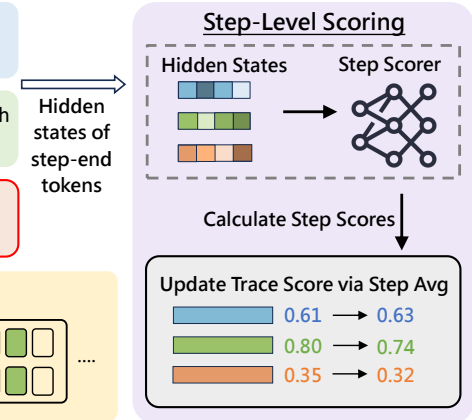


Figure 3: Overview of the STEP framework. The step-level scoring module extracts hidden states at step boundaries and uses a trained step scorer to compute step-level scores, which are averaged to obtain trace-level scores. The KV-cache monitor triggers pruning when GPU memory is saturated, removing the trace with the lowest score and releasing its KV cache to prevent queuing delays.

reasoning quality at each step.

Step Representation Following common practice (Yang et al., 2025c), we extract the reasoning content between “<think>” and “</think>”, and segment it into N reasoning steps using “\n\n” as the delimiter. Then a trace is defined as: $t = (s_1, s_2, \dots, s_N)$. For each step s_n , we use the last-layer hidden state of step-end token¹ \mathbf{h}_n ($\mathbf{h}_n \in \mathbb{R}^d$ where d is the hidden dimension of LLM.) as input to the scorer, as it accumulates contextual information from all previous reasoning steps in the trace.

Label Construction As supervision for the step scorer, we propagate the trace-level correctness label $y \in \{0, 1\}$ to all steps within the trace as pseudo-labels for simplicity, as fine-grained step-level annotation is costly to obtain. Specifically,

$$\tilde{y}_n = y, \quad \forall n \in \{1, \dots, N\},$$

where $y = 1$ indicates a correct trace and $y = 0$ an incorrect one. For training data curation, we balance the number of correct and incorrect traces, while including all steps from each trace in the training set. Details of the training data are provided in Section 5.1.

Model Architecture The step scorer f_θ is a two-layer MLP, which we find sufficient for capturing quality signals from hidden states. It maps \mathbf{h}_n to a

correctness probability score \hat{y}_n :

$$\hat{y}_n = f_\theta(\mathbf{h}_n) = \sigma(\mathbf{W}_2 \text{ReLU}(\mathbf{W}_1 \mathbf{h}_n + \mathbf{b}_1) + \mathbf{b}_2),$$

where $\mathbf{W}_1 \in \mathbb{R}^{m \times d}$, $\mathbf{W}_2 \in \mathbb{R}^{1 \times m}$, $\mathbf{b}_1 \in \mathbb{R}^m$, and $\mathbf{b}_2 \in \mathbb{R}$ are trainable parameters, with m denoting the hidden dimension of the MLP. The function $\sigma(\cdot)$ denotes the sigmoid activation.

Training Objective We train the step scorer using a weighted binary cross-entropy loss:

$$\mathcal{L} = -\frac{1}{N} \sum_{n=1}^N \left(\alpha \tilde{y}_n \log \hat{y}_n + (1 - \tilde{y}_n) \log (1 - \hat{y}_n) \right),$$

where $\alpha = K^-/K^+$ is the ratio of negative to positive samples in the training data. This weighting compensates for the imbalance at the step level, as incorrect traces tend to be longer and thus generate more negative step instances, even when the dataset is balanced at the trace level.

4.2 Memory Constraint as Trigger

The timing of pruning is critical for improving generation efficiency. Prior approaches typically rely on predefined confidence thresholds (Fu et al., 2025) or fixed wall-clock schedules (Hong et al., 2025) to trigger pruning, without considering the behavior of inference system. While these methods reduce generation time by terminating unpromising traces that may produce longer sequences, they overlook a more fundamental bottleneck revealed

¹It refers to any token whose text contains “\n\n”.

in Section 3: the excessive waiting time caused by GPU memory constraints. As a result, existing methods fail to address the dominant source of inefficiency during inference.

To overcome this limitation, we propose a memory-triggered pruning mechanism. Whenever GPU memory is full, and the KV cache for the next decoding step cannot be scheduled, we immediately prune the trace with the lowest trace level score and release its KV cache. This design completely eliminates waiting queues, thereby avoiding prolonged suspension and repeated resumption of traces. Moreover, our mechanism is free of additional hyperparameters, making it simple and robust in practice.

4.3 Pruning with STEP

With the building blocks for *when* and *how* to prune in place, we now describe the overall algorithm. Given an input prompt, we generate T reasoning traces in parallel. During generation, whenever a trace t produces a step-end token that signals the end of a reasoning step, we compute a step-level score \hat{y}_n^t by applying the step scorer to the corresponding hidden state. The trace-level score is then defined as the mean of all step-level scores of this trace accumulated so far:

$$score_t = \frac{1}{n} \sum_{i=1}^n \hat{y}_i^t,$$

where n denotes the number of reasoning steps currently generated in trace t . Compared to relying solely on the score of the most recent step, this aggregated score provides a more stable estimate of trace quality by capturing the evolution of the reasoning process across steps. In particular, it mitigates the variance of individual step scores and reflects whether a trace consistently follows a coherent reasoning trajectory.

During generation, whenever GPU memory becomes full due to KV cache usage, we prune the trace with the lowest trace-level score, thereby releasing memory for more promising traces. Once all reasoning traces have either completed generation or been pruned, we collect the outputs of the completed traces and perform weighted voting based on their final trace-level scores to aggregate the final answer. The pseudo-code for STEP is shown in Algorithm 1.

Algorithm 1: STEP

```

Input: Problem  $P$ , step scorer  $f(\cdot)$ , trace budget  $N$ 
Output: Final answer  $\hat{a}$ 
 $\mathcal{T} \leftarrow \text{INITTRACES}(P, N)$ 
while  $\mathcal{T} \neq \emptyset$  do
  foreach trace  $t \in \mathcal{T}$  do
     $(x, h) \leftarrow \text{NEXTTOKEN}(t);$ 
    if "\n\n" in  $x$  then
       $\hat{y} \leftarrow f(h);$ 
      Update  $score_t$  with  $\hat{y}$ 
    if GPUMEMORYFULL then
       $t^* \leftarrow \arg \min_{t \in \mathcal{T}} score_t;$ 
      RELEASEKVCACHE( $t^*$ );
       $\mathcal{T} \leftarrow \mathcal{T} \setminus \{t^*\};$ 
  end
   $\hat{a} \leftarrow \text{WEIGHTEDVOTE}(\mathcal{T}, \{score_t\});$ 
return  $\hat{a};$ 

```

5 Experiment

In this section, we conduct comprehensive experiments to evaluate the effectiveness of our method, demonstrating improvements in both reasoning quality and generation efficiency. We further analyze its performance under different settings and investigate the underlying factors contributing to these improvements.

5.1 Experiment Setup

Models We evaluate on three reasoning LLMs: Qwen3-4B-Thinking-2507 (Yang et al., 2025a), DeepSeek-R1-0528-Qwen3-8B (DeepSeek-AI, 2025), and Phi-4-reasoning-plus(14B) (Abdin et al., 2025). These models are selected for their strong mathematical reasoning and long-chain-of-thought capabilities, and are fully open-sourced to ensure reproducibility.

Benchmarks We evaluate on four challenging datasets: AIME-25 (Art of Problem Solving, 2025), HMMT-24 (HMMT, 2024), HMMT-25 (HMMT, 2025), and GPQA-Diamond (Rein et al., 2024). The first three comprise high-difficulty mathematical competition problems, while GPQA consists of graduate-level reasoning tasks in general science.

Baselines We compare our method against the following baseline methods:

- **Chain-of-Thought (CoT)** (Wei et al., 2022) uses standard CoT prompting, where the model generates a single reasoning trajectory that directly leads to the final answer.
- **Self-Consistency (SC)** (Wang et al., 2022) generates N independent reasoning traces and

Methods	AIME-25			HMMT-24			HMMT-25			GPQA-D		
	Acc. \uparrow	Token \downarrow	Lat. \downarrow	Acc. \uparrow	Token \downarrow	Lat. \downarrow	Acc. \uparrow	Token \downarrow	Lat. \downarrow	Acc. \uparrow	Token \downarrow	Lat. \downarrow
<i>Qwen3-4B-Thinking-2507</i>												
CoT	81.3	22.7	145	47.5	29.8	194	55.8	26.8	174	65.8	8.9	54
SC	86.7	1454.3	1430	50.8	1905.5	2277	65.0	1714.3	1833	68.1	569.1	252
Slim-SC	86.7	957.5	767	50.0	1002.6	1025	65.8	930.8	848	64.9	414.7	236
DeepConf	90.0	841.5	933	56.7	1069.4	1373	68.3	1037.0	1253	67.6	379.1	257
STEP	88.3	1131.5	675	58.3	1149.3	979	70.0	1109.8	732	68.5	539.6	223
<i>DeepSeek-R1-0528-Qwen3-8B</i>												
CoT	77.5	26.4	204	50.0	33.1	307	60.4	29.9	256	62.3	11.4	81
SC	83.3	1691.0	2259	55.8	2116.2	3102	70.0	1913.0	2680	67.1	729.8	484
Slim-SC	83.3	1519.9	1960	55.0	1830.7	2789	69.2	1733.2	2388	66.2	564.1	424
DeepConf	81.7	916.4	1475	56.7	1084.2	1791	71.7	993.1	1540	68.7	419.8	409
STEP	85.0	989.7	891	59.2	1105.8	1116	73.3	1087.2	1006	68.2	635.7	378
<i>Phi-4-reasoning-plus</i>												
CoT	78.3	16.0	194	51.7	21.2	294	58.6	21.7	246	69.5	11.9	105
SC	86.7	1026.7	1687	56.7	1356.4	2405	75.0	1389.8	2529	76.3	762.5	1081
Slim-SC	85.0	875.8	1354	55.0	1178.9	1918	74.2	1120.4	1690	72.3	560.6	655
DeepConf	85.8	537.2	1165	57.5	714.9	1523	75.0	755.6	1770	74.8	401.9	1285
STEP	87.5	503.4	519	58.3	579.8	630	75.8	585.2	643	76.7	441.5	445

Table 1: Main experimental results comparing our method with baseline methods (CoT, SC, Slim-SC, and DeepConf) on various models and benchmarks. Evaluation metrics include accuracy (%), average token usage ($\times 10^3$), and inference latency (s).

determines the final answer by majority voting on the predicted solutions.

- **Slim-SC** (Hong et al., 2025) proposes a step-wise thought pruning strategy for self-consistency: it detects and removes redundant reasoning chains by measuring inter-chain similarity at the thought level, reducing latency while maintaining accuracy.
- **DeepConf** (Fu et al., 2025) utilizes the model’s internal confidence signals to monitor the quality of each reasoning trace during generation, allowing dynamic termination of unpromising traces. The final answer is decided by confidence-weighted voting.

Implementation Details To train the step scorer, we curated a dataset of mathematical problems from HMMT 2012–2023 (HMMT, 2012–2023), which provide diverse examples for learning hidden state representations indicative of reasoning quality. We sampled 64 solutions from the target model for each problem and verified their correctness using a deterministic rule-based verifier. We then randomly selected 5,000 correct and 5,000 incorrect traces to form a balanced training set. More details are shown in Appendix A.

We evaluate all methods under the sampling budget of $N = 64$. For Slim-SC, we apply random pruning with a similarity threshold of 0.95

as recommended in the original work (Hong et al., 2025). For DeepConf, we use the online variant (DeepConf-low) with $N_{\text{init}} = 16$ traces for offline warmup, then generate the remaining 48 traces with early termination for those falling below the top-10% confidence threshold. All experiments are conducted using a modified vLLM (Kwon et al., 2023) framework with our pruning algorithm on a single 96GB NVIDIA GH200 GPU. More detailed settings are provided in the Appendix B.

5.2 Main Results

Tab. 1 presents the main experimental results comparing our method against baseline approaches across four benchmarks and three reasoning models. We report accuracy, average output token usage, and latency per problem as evaluation metrics.

Consistent Accuracy Improvements Our method achieves the highest accuracy on most of the benchmark-model combinations. On mathematical reasoning benchmarks, our approach consistently outperforms SC, Slim-SC, and DeepConf across all three models. For example, on HMMT-25, our method improves accuracy by 5.0%, 3.3%, and 0.8% over SC for Qwen3-4B-Thinking-2507, DeepSeek-R1-0528-Qwen3-8B, and Phi-4-reasoning-plus, respectively. For the general science reasoning benchmark GPQA-Diamond, our method also achieves competitive

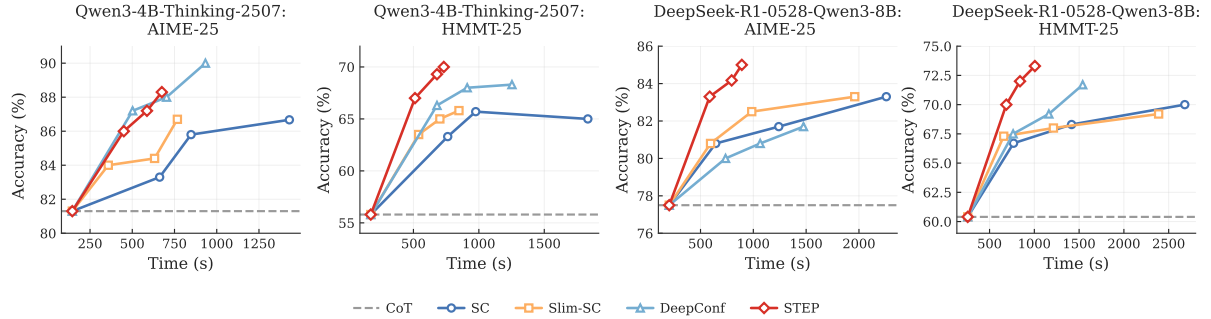


Figure 4: Latency scaling comparison between STEP and baseline methods on AIME-25 and HMMT-25 using Qwen3-4B-Thinking-2507 and DeepSeek-R1-0528-Qwen3-8B.

accuracy across all models, demonstrating its generalizability beyond mathematical domains. We attribute STEP’s accuracy improvements to our hidden-state-based step scorer, which provides accurate estimation of trace quality during generation, enabling effective pruning of unpromising traces and reliable answer aggregation through weighted voting. We provide a detailed analysis of our step scorer’s ranking ability in Section 5.3.2.

Superior Computational Efficiency A key advantage of our method lies in end-to-end latency improvement. Compared to SC, our approach reduces latency by 45%–70% on average across different settings. For instance, on Phi-4-reasoning-plus with HMMT-24, our method achieves 58.3% accuracy in just 630 seconds, compared to 2405 seconds for SC, yielding a 3.8 \times speedup. Even compared to Slim-SC and DeepConf, our method consistently achieves lower latency while maintaining comparable or superior accuracy. On DeepSeek-R1-0528-Qwen3-8B with AIME-25, our approach reduces latency from 1475s (DeepConf) to 891s, a 1.7 \times speedup, while achieving higher accuracy. And from result of average output token length, we observe that our method consistently reduces the token counts compared with SC across all models and benchmarks, while keeping a comparable level of tokens with DeepConf and Slim-SC. These results reveal that eliminating waiting queue significantly contributes to accelerating generation. We present a detailed analysis of acceleration at Section 5.3.3.

5.3 Analysis

5.3.1 Latency Scaling

To verify the effectiveness and efficiency of STEP under varying computational budgets, we conduct latency scaling experiments using Qwen3-4B-Thinking-2507 and DeepSeek-R1-0528-Qwen3-8B

on AIME-25 and HMMT-25. We set the sampling budget to 16, 32, and 64, and evaluate our method against baseline approaches. Since larger budgets increase both latency and potential accuracy, this setup allows us to examine accuracy-latency trade-offs across different computational regimes.

As illustrated in Fig. 4, STEP achieves superior accuracy-latency trade-offs in most settings, reaching higher accuracy at any given time budget. For instance, on Qwen3-4B-Thinking-2507 with HMMT-25, STEP achieves 70% accuracy using around 40% of the latency required by SC, which reaches just 65% accuracy. Similarly, on DeepSeek-R1-0528-Qwen3-8B with AIME-25, our method attains 85% accuracy while consuming approximately 40% of the latency that SC requires to achieve comparable performance. Compared to Slim-SC and DeepConf, which also aim to reduce inference cost, our method still demonstrates clear advantages. On HMMT-25, our method consistently outperforms both Slim-SC and DeepConf across all time budgets, achieving higher accuracy with lower latency. These results demonstrate that our method exhibits favorable latency scaling properties, outperforming the baseline methods across different models and datasets.

5.3.2 Ranking Ability of Step Scorer

Beyond overall efficiency, we examine whether our step scorer can reliably identify promising traces. We evaluate its discriminative ability against token-level confidence, as used in DeepConf. We conduct experiments on 256 reasoning traces per question generated by Qwen3-4B-Thinking-2507 on AIME-25 and HMMT-25. For each trace, we input only the first $k\%$ of steps and compute an average score. We compare against mean token-level confidence computed from the same partial trace. We adopt pairwise ranking accuracy (RankAcc) as

our evaluation metric. For each question q with a set of correct traces \mathcal{P}_q and incorrect traces \mathcal{N}_q , RankAcc measures the proportion of correctly ordered positive–negative pairs:

$$\text{RankAcc} = \mathbb{E}_{q \in Q} \left[\mathbb{E}_{p \in \mathcal{P}_q, n \in \mathcal{N}_q} [\mathbb{1}[s(p) > s(n)]] \right],$$

where $s(\cdot)$ denotes the scoring function.

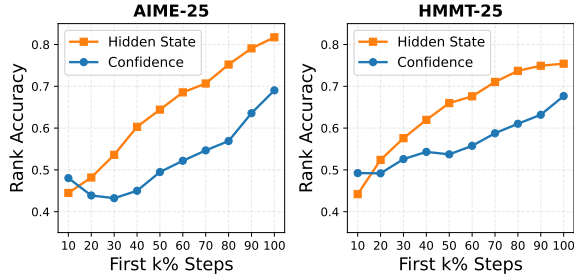


Figure 5: Pairwise RankAcc of the hidden-state-based step scorer versus token-level confidence.

As shown in Fig. 5, the hidden-state-based step scorer outperforms token confidence, and its discriminative performance improves steadily as more reasoning steps become available. Even at early stages, the step scorer already achieves strong ranking accuracy, demonstrating that hidden states encode rich information about solution correctness well before the final answer is reached. We also include a visualization of trace-level score dynamics from hidden-state-based step scorer in Appendix E.

5.3.3 Profiling Acceleration by Pruning

The acceleration of STEP stems from two complementary factors: reducing the number of generated tokens and eliminating waiting time during generation. Token counts are reported in Tab. 1. We further conduct experiments, profiling the end-to-end generation time breakdown of DeepSeek-R1-0528-Qwen3-8B on HMMT25 with 64 traces, and results are reported in Tab. 2. DeepConf consists of two consecutive stages with $N=16$ in warmup and $N=48$ in pruning stage, and we report them separately. We observe that all pruning methods decrease generated tokens compared with SC, and lead to lower decoding time in Tab. 2. Beyond token-level efficiency, the key distinction lies in how to handle waiting time. DeepConf and Slim-SC reduce waiting time compared to SC, since pruning naturally alleviates GPU memory pressure, thus shortening the waiting queue. However, their pruning decisions are not explicitly tied to GPU memory usage, and therefore cannot fully eliminate the waiting time. In contrast, our method

Method	SC	DeepConf		Slim-SC	STEP
		Warmup	Prune		
Wait	1526	69	194	1155	0
Decode	1256	680	726	983	1024

Table 2: Waiting time and decoding time (in seconds) comparison across different methods.

completely removes waiting queue by triggering pruning in a memory-aware manner, resulting in the lowest end-to-end generation latency.

Taken together, these results demonstrate that while reducing generated tokens lowers decoding overhead, explicitly eliminating waiting time is critical for further accelerating end-to-end generation.

5.3.4 GPU memory sensitivity

STEP triggers pruning when KV cache saturates GPU memory. Since smaller GPU memory budgets lead to earlier pruning, it is important to examine the robustness of our method under different memory constraints. To this end, we conduct a sensitivity analysis by varying the maximum GPU memory utilization from 0.5 to 0.9, on a 96GB NVIDIA GH200 GPU. We report results on the HMMT-25 using DeepSeek-R1-0528-Qwen3-8B, sampling 32 reasoning traces per problem. The results are summarized in Tab. 3.

Memory	0.5	0.6	0.7	0.8	0.9
Accuracy	70.0	69.1	70.0	68.3	73.3

Table 3: Accuracy result under different GPU memory utilization settings.

We observe that the accuracy remains stable across different memory budgets ($70.1 \pm 1.8\%$). Even under smaller GPU memory budgets, where pruning is triggered earlier, our method consistently achieves strong performance. This observation is consistent with the findings in Section 5.3.2, which show that our scorer is able to identify promising reasoning traces at an early stage of generation. These results suggest that our method is insensitive to GPU memory.

6 Conclusion

In this work, we introduce STEP, a method that combines hidden-state-based trace evaluation with GPU-memory-aware pruning for efficient test-time scaling. By leveraging early reasoning signals and system-level optimization, STEP achieves

45%–70% latency reduction while improving accuracy, demonstrating the potential of efficient parallel scaling for complex reasoning tasks.

Limitations

Our work has two primary limitations. First, the step scorer relies on pseudo-labels generated by propagating trace-level correctness to individual steps. Such weak supervision is inherently noisy and may compromise robustness under domain shift or when traces contain steps of varying quality. Second, the most significant latency improvements depend on memory-triggered pruning, which is tightly coupled to the serving infrastructure. While we observe consistent speedups across different memory budgets, the exact magnitude may differ across inference engines, multi-GPU configurations, and alternative memory management strategies.

Acknowledgments

This research was supported by the National Science Foundation (NSF) under Grant No. 2441601. The work utilized the Delta and DeltaAI system at the National Center for Supercomputing Applications (NCSA) and Jetstream2 at Indiana University through allocation CIS240055 from the Advanced Cyberinfrastructure Coordination Ecosystem: Services & Support (ACCESS) program, which is supported by National Science Foundation grants #2138259, #2138286, #2138307, #2137603, and #2138296. The Delta advanced computing resource is a collaborative effort between the University of Illinois Urbana-Champaign and NCSA, supported by the NSF (award OAC 2005572) and the State of Illinois. UIUC SSAIL Lab is supported by research funding and gift from Google, IBM, Amazon, and AMD.

References

Marah Abdin, Sahaj Agarwal, Ahmed Awadallah, Vidhisha Balachandran, Harkirat Behl, Lingjiao Chen, Gustavo de Rosa, Suriya Gunasekar, Mojan Javaheripi, Neel Joshi, Piero Kauffmann, Yash Lara, Caio César Teodoro Mendes, Arindam Mitra, Bessmira Nushi, Dimitris Papailiopoulos, Olli Saarikivi, Shital Shah, Vaishnavi Shrivastava, and 4 others. 2025. *Phi-4-reasoning technical report*. *Preprint*, arXiv:2504.21318.

Art of Problem Solving. 2025. Aime 2025 problems and solutions. https://artofproblemsolving.com/wiki/index.php?title=2025_AIME_I_Problems.

Prateek Chhikara. 2025. *Mind the confidence gap: Overconfidence, calibration, and distractor effects in large language models*. *Preprint*, arXiv:2502.11028.

DeepSeek-AI. 2025. *Deepseek-r1: Incentivizing reasoning capability in llms via reinforcement learning*. *Preprint*, arXiv:2501.12948.

Yichao Fu, Xuewei Wang, Yuandong Tian, and Jiawei Zhao. 2025. *Deep think with confidence*. *Preprint*, arXiv:2508.15260.

HMMT. 2012–2023. *Hmm problems archive (2012–2023)*. HMMT Official Archive.

HMMT. 2024. *Archive of february 2024*. HMMT Official Archive.

HMMT. 2025. *Archive of february 2025*. HMMT Official Archive.

Colin Hong, Xu Guo, Anand Chaanan Singh, Esha Choukse, and Dmitrii Ustjugov. 2025. *Slim-SC: Thought pruning for efficient scaling with self-consistency*. In *Proceedings of the 2025 Conference on Empirical Methods in Natural Language Processing*, pages 34488–34505, Suzhou, China. Association for Computational Linguistics.

Zhenyu Hou, Xin Lv, Rui Lu, Jiajie Zhang, Yujiang Li, Zijun Yao, Juanzi Li, Jie Tang, and Yuxiao Dong. 2025. *T1: Advancing language model reasoning through reinforcement learning and inference scaling*. In *Forty-second International Conference on Machine Learning*.

Shiyu Ji, Yixuan Wang, Yijun Liu, Qingfu Zhu, and Wanxiang Che. 2025. *Seer self-consistency: Advance budget estimation for adaptive test-time scaling*. *Preprint*, arXiv:2511.09345.

Zhewei Kang, Xuandong Zhao, and Dawn Song. 2025. *Scalable best-of-n selection for large language models via self-certainty*. *Preprint*, arXiv:2502.18581.

Jared Kaplan, Sam McCandlish, Tom Henighan, Tom B Brown, Benjamin Chess, Rewon Child, Scott Gray, Alec Radford, Jeffrey Wu, and Dario Amodei. 2020. Scaling laws for neural language models. *arXiv preprint arXiv:2001.08361*.

Takeshi Kojima, Shixiang Shane Gu, Machel Reid, Yutaka Matsuo, and Yusuke Iwasawa. 2023. *Large language models are zero-shot reasoners*. *Preprint*, arXiv:2205.11916.

Woosuk Kwon, Zhuohan Li, Siyuan Zhuang, Ying Sheng, Lianmin Zheng, Cody Hao Yu, Joseph Gonzalez, Hao Zhang, and Ion Stoica. 2023. Efficient memory management for large language model serving with pagedattention. In *Proceedings of the 29th symposium on operating systems principles*, pages 611–626.

Zhenwen Liang, Ruosen Li, Yujun Zhou, Linfeng Song, Dian Yu, Xinya Du, Haitao Mi, and Dong Yu. 2025. *Clue: Non-parametric verification from experience via hidden-state clustering*. *Preprint*, arXiv:2510.01591.

OpenAI. 2024a. *Gpt-4 technical report*. *Preprint*, arXiv:2303.08774.

OpenAI. 2024b. Learning to reason with llms. <https://openai.com/index/learning-to-reason-with-llms/>.

David Rein, Betty Li Hou, Asa Cooper Stickland, Jackson Petty, Richard Yuanzhe Pang, Julien Dirani, Julian Michael, and Samuel R. Bowman. 2024. *Gpqa: A graduate-level google-proof q&a benchmark*. In *Conference on Language Modeling (COLM) 2024*.

Shangqing Tu, Yaxuan Li, Yushi Bai, Lei Hou, and Juanzi Li. 2025. *Deeprune: Parallel scaling without inter-trace redundancy*. *Preprint*, arXiv:2510.08483.

Xuezhi Wang, Jason Wei, Dale Schuurmans, Quoc Le, Ed Chi, Sharan Narang, Aakanksha Chowdhery, and Denny Zhou. 2022. Self-consistency improves chain of thought reasoning in language models. *arXiv preprint arXiv:2203.11171*.

Zili Wang, Tianyu Zhang, Haoli Bai, Lu Hou, Xianzhi Yu, Wulong Liu, Shiming Xiang, and Lei Zhu. 2025. *Faster and better LLMs via latency-aware test-time scaling*. In *Findings of the Association for Computational Linguistics: EMNLP 2025*, pages 17124–17137, Suzhou, China. Association for Computational Linguistics.

Jason Wei, Xuezhi Wang, Dale Schuurmans, Maarten Bosma, Fei Xia, Ed Chi, Quoc V Le, Denny Zhou, and 1 others. 2022. Chain-of-thought prompting elicits reasoning in large language models. *Advances in neural information processing systems*, 35:24824–24837.

An Yang, Anfeng Li, Baosong Yang, Beichen Zhang, Binyuan Hui, Bo Zheng, Bowen Yu, Chang Gao, Chengen Huang, Chenxu Lv, Chujie Zheng, Dayiheng Liu, Fan Zhou, Fei Huang, Feng Hu, Hao Ge, Haoran Wei, Huan Lin, Jialong Tang, and 41 others. 2025a. *Qwen3 technical report*. *Preprint*, arXiv:2505.09388.

An Yang, Baosong Yang, Binyuan Hui, Bo Zheng, Bowen Yu, Chang Zhou, Chengpeng Li, Chengyuan Li, Dayiheng Liu, Fei Huang, and 1 others. 2024. *Qwen2 technical report*. *arXiv preprint arXiv:2407.10671*.

Rubing Yang, Huajun Bai, Song Liu, Guanghua Yu, Runzhi Fan, Yanbin Dang, Jiebing Zhang, Kai Liu, Jianchen Zhu, and Peng Chen. 2025b. *Specexit: Accelerating large reasoning model via speculative exit*. *Preprint*, arXiv:2509.24248.

Wang Yang, Xiang Yue, Vipin Chaudhary, and Xiaotian Han. 2025c. Speculative thinking: Enhancing small-model reasoning with large model guidance at inference time. *arXiv preprint arXiv:2504.12329*.

Anqi Zhang, Yulin Chen, Jane Pan, Chen Zhao, Aurojit Panda, Jinyang Li, and He He. 2025. *Reasoning models know when they’re right: Probing hidden states for self-verification*. In *Second Conference on Language Modeling*.

Lianmin Zheng, Liangsheng Yin, Zhiqiang Xie, Chuyue Sun, Jeff Huang, Cody Hao Yu, Shiyi Cao, Christos Kozyrakis, Ion Stoica, Joseph E. Gonzalez, Clark Barrett, and Ying Sheng. 2024. *SGLang: Efficient execution of structured language model programs*. In *The Thirty-eighth Annual Conference on Neural Information Processing Systems*.

Zhi Zhou, Tan Yuhao, Zenan Li, Yuan Yao, Lan-Zhe Guo, Xiaoxing Ma, and Yu-Feng Li. 2025. *Bridging internal probability and self-consistency for effective and efficient llm reasoning*. *Preprint*, arXiv:2502.00511.

A Step Scorer Training

A.1 Training Parameters

The training hyper-parameters used in the training process of step scorer are listed in Tab. 4.

Parameter	Value
MLP Structure	Input → 512 (ReLU) → 1
Batch Size	128
Max Epochs	20
Early Stopping Patience	5
Learning Rate	1×10^{-4}
Weight Decay	1×10^{-5}
Optimizer	Adam
Loss Function	BCEWithLogitsLoss

Table 4: Training Parameters

The input dimension corresponds to the hidden state size of each LLM: 2560 (Qwen3-4B-Thinking-2507), 4096 (DeepSeek-R1-0528-Qwen3-8B), and 5120 (Phi-4-reasoning-plus).

A.2 Training Dataset

For training the step scorer, we constructed a dataset comprising mathematical problems from HMMT 2012–2023 (HMMT, 2012–2023). We specifically utilized problems from the February competition in Algebra, Combinatorics, and Geometry, which provide diverse and challenging examples for learning hidden state representations indicative of reasoning quality.

We sampled 64 solutions from the corresponding LLM for each problem and verified the correctness of their final answers using a deterministic

rule-based verifier adapted from the Qwen2.5-Math project (Yang et al., 2024). The verifier normalizes answer strings and checks correctness against the ground truth via numeric matching and SymPy-based symbolic equivalence. We then randomly selected 5,000 correct and 5,000 incorrect traces to form a balanced training set for each LLM.

B Experimental Settings

B.1 Sampling Parameters

The sampling parameters used for each model across all experiments are listed in Tab. 5. Temperature, top-p, top-k, and maximum generation length remain fixed for all methods. Here, Qwen3-4B refers to Qwen3-4B-Thinking-2507 and Deepseek-8B refers to DeepSeek-R1-0528-Qwen3-8B.

Model	Temperature	Top-p	Top-k	Max gen len
Qwen3-4B	0.6	0.95	20	64k
DeepSeek-8B	0.6	0.95	20	64k
Phi-4-reasoning-plus	0.8	0.95	50	32k

Table 5: Sampling Parameters

B.2 Prompt Templates

We apply the following prompt template to each problem in the test benchmarks for all methods.

Prompt Template

Please reason step by step, and put your final answer within \boxed{ }.
Question: {question_text}

B.3 Baselines

- **Slim-SC:** We use the Random Pruning (RP) strategy in the original paper since it provides a clear advantage in inference speed while retaining accuracy.
- **DeepConf:** We use the online variant (DeepConf-low), where traces are terminated when their confidence falls below the level that retains the top 10% highest-confidence traces from the warmup phase. We set $N_{\text{init}} = 16$ warmup traces for $N \in \{32, 64\}$ and $N_{\text{init}} = 8$ for $N = 16$.

C System Integration

STEP is built upon the implementation logic of vLLM-V1, where the engine core and model runner reside in separate processes. We place the step

scorer on the same GPU and execute its running logic within the same process as the model runner. Only the scores are passed via inter-process communication to the engine core, where the scheduler performs pruning decisions. The experimental environment is configured as follows:

- **vLLM:** 0.11.1
- **Python:** 3.12
- **CUDA:** 12.4

D Additional Computational Overhead

The step scorer is implemented as an auxiliary MLP, which inevitably introduces additional computation. Since this MLP is invoked at every reasoning step, we quantify its overhead by comparing the per-step computation cost of the scorer with that of the underlying LLM.

We approximate the FLOPs of one forward generation step of the LLM as $2N$, where N denotes the number of non-embedding parameters (Kaplan et al., 2020). The computation cost of the step-level MLP is $2m(d + 1)$, where m is the hidden dimension of the MLP and d is the hidden dimension of the LLM. The relative overhead per step is therefore

$$\frac{2m(d + 1)}{2N * t},$$

where t is the average tokens per step. In practice, we set $m = 512$, d is on the order of 10^3 , N is on the order of billions, and t is around 10^2 . Under these settings, the resulting ratio is below 10^{-6} , indicating that the computational overhead introduced by the step scorer is negligible.

E Trace-level Score Dynamics

We visualize trace-level score dynamics on AIME-25 for Qwen3-4B-Thinking-2507 and DeepSeek-R1-0528-Qwen3-8B in Fig. 6 and Fig. 7. Each subplot shows the prefix mean of step scores as a function of token position (grouped into 1024-token bins), where the green and red lines represent the average scores across correct and incorrect traces, respectively. Solutions are generated with $N=64$ samples per problem. The results demonstrate that our step scorer effectively separates promising reasoning paths from unpromising ones throughout generation.

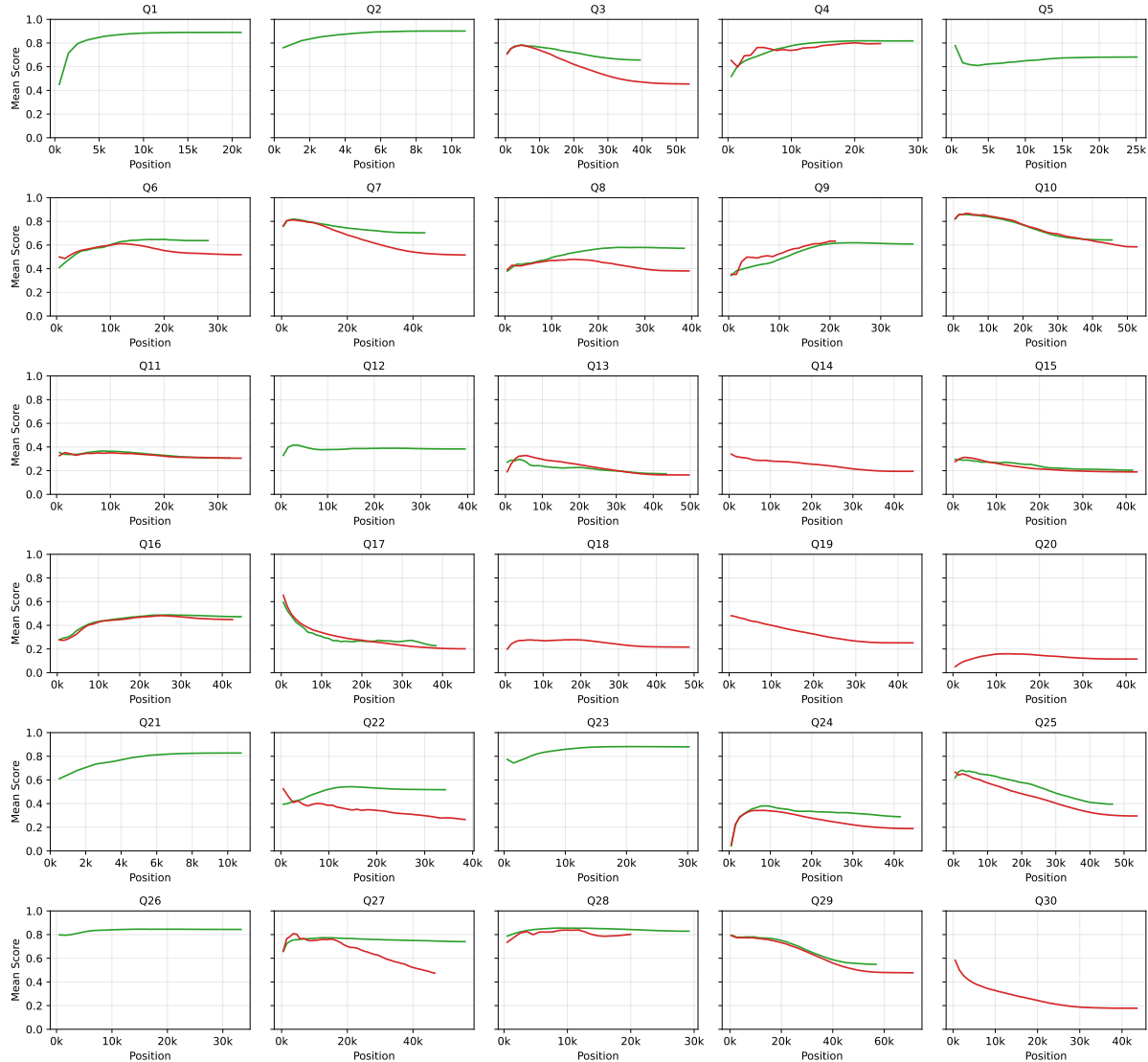


Figure 6: Trace-level score dynamics on AIME-25 for Qwen3-4B-Thinking-2507.

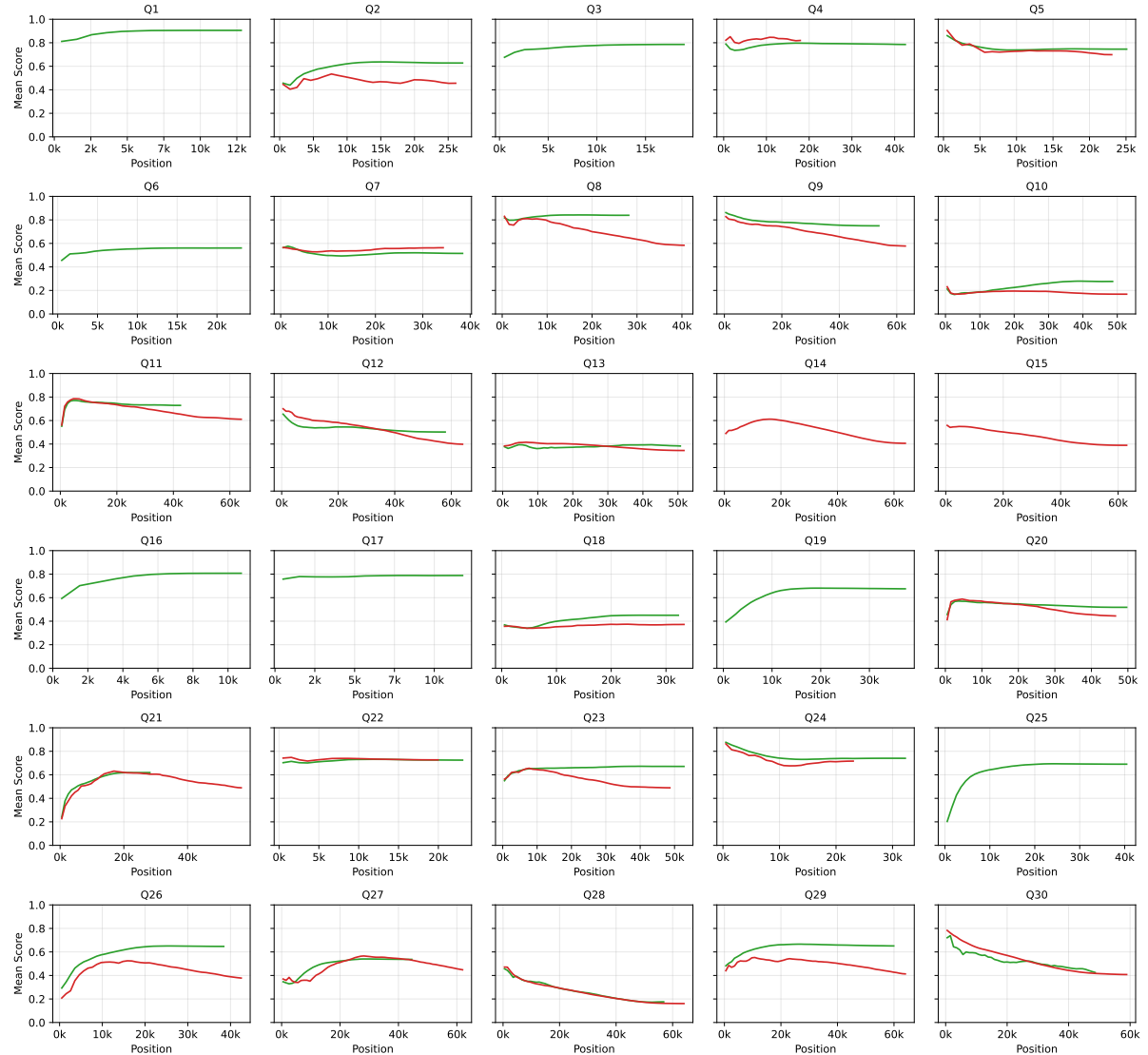


Figure 7: Trace-level score dynamics on AIME-25 for DeepSeek-R1-0528-Qwen3-8B.